



Dedicated to the memory of  
Professor Candin Liteanu on his 100<sup>th</sup> anniversary

## SPECTROSCOPIC AND THERMAL STUDIES ON THE IRON(III) MERCAPTO-THIADIAZOL-THIOSUCCINATE PRECURSOR FOR IRON(III) OXIDES

Monica M. VENTER,<sup>a,\*</sup> Firuța GOGA,<sup>a</sup> Vasile N. BERCEAN,<sup>b</sup> Mircea NASUI,<sup>c</sup> and Gheorghe BORODI<sup>d</sup>

<sup>a</sup>“Babeș-Bolyai” University, Faculty of Chemistry and Chemical Engineering, 11 Arany Janos, 400028 Cluj-Napoca, Roumania

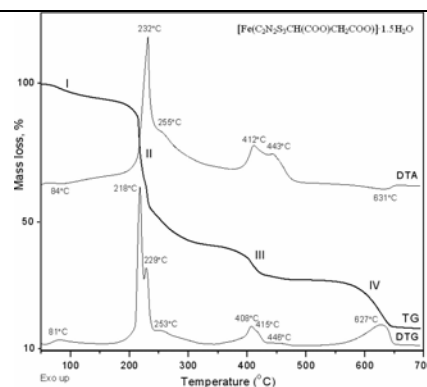
<sup>b</sup>“Politehnica” University, Faculty of Industrial Chemistry and Environment Engineering, 6 Vasile Pârvan, 300223 Timișoara, Roumania

<sup>c</sup> Technical University, Center for Superconductivity, Spintronics and Surface Science, 28 Memorandumului, 400114 Cluj-Napoca, Roumania

<sup>d</sup>National Institute for Research and Development of Isotopic and Molecular Technologies, 65-103 Donath, 400293 Cluj-Napoca, Roumania

Received September 29, 2014

Reaction of the new (3*H*-2-thioxo-1,3,4-thiadiazol-5-yl)-thiosuccinic acid (H<sub>3</sub>L) with FeCl<sub>3</sub>·6H<sub>2</sub>O and Et<sub>3</sub>N in aqueous medium produced a new iron(III) complex [FeL]·1.5H<sub>2</sub>O, regardless the molar ratio of the reagents. The empirical formula of the product is supported by elemental analysis. Both acid and complex are characterized by vibrational spectroscopy (FT-IR, FT-Raman). The spectra are consistent with the complete deprotonation of the acid and the formation of the product. The TGA/DTA/DTG analysis of [FeL]·1.5H<sub>2</sub>O indicates the thermolysis of the precursor in four major steps, to produce α-Fe<sub>2</sub>O<sub>3</sub>. Each solid residue is monitored by FT-IR spectroscopy. The identity of the final thermolysis product is confirmed by powder X-ray diffraction.



### INTRODUCTION

Iron(III) oxide, Fe<sub>2</sub>O<sub>3</sub> is known in its four crystalline forms α-hematite, β, γ-maghemite and ε. Among them, α and γ are well known materials with outstanding properties and multiple applications. Moreover, Producing Fe<sub>2</sub>O<sub>3</sub> as nanoparticles (NP) enhances the surface effect, induces new properties or improves the existing ones. Thus, maghemite is used in information storage, ferrofluids, various magnetic devices and

biotechnology, mainly due to its magnetic properties. On the other hand, hematite is the most eco-friendly and the most air stable polymorph, and finds multiple applications as gas sensor, catalyst, pigment, ingredient on Li-ion batteries etc.<sup>1-3</sup>

Iron(III) oxide NP can be obtained from solid state or solution (wet chemical methods). In all cases, the structure and reactivity of the precursors as well as the preparation technique are of great importance for the formation of the advanced

\* Corresponding author: monica@chem.ubbcluj.ro

material. For example, hydrolysis of iron(III) inorganic salts or metal-organic derivatives may produce  $\alpha$ -Fe<sub>2</sub>O<sub>3</sub> in hydrothermal conditions,<sup>4</sup> microwave-assisted<sup>5,6</sup> or by sonolysis.<sup>7</sup> The presence of capping agents in the solution helps producing mono-dispersed NP by preventing agglomeration. Thus, Fe<sub>2</sub>O<sub>3</sub> NP of 6-30 nm were obtained by capping with oleic acid and related compounds.<sup>8,9</sup> However, capping may not be desirable for applications such as catalysis, due to active site obstruction by capping molecules.<sup>10</sup> Alternatively, preparation of Fe<sub>2</sub>O<sub>3</sub> NP in solid state involves mainly thermal decomposition of iron carboxylates. These precursors may be obtained by direct complexation of the carboxylic acid with iron cations, or by in situ oxidation of polyols followed by complexation of the resulting poly-acids.<sup>2,3,11</sup> Thermal decomposition of iron carboxylates in air produces  $\alpha$  or  $\gamma$ -Fe<sub>2</sub>O<sub>3</sub> while thermolysis in inert atmosphere may lead to Fe<sub>3</sub>O<sub>4</sub> (magnetite) or metallic iron.<sup>12</sup>

The aim of this work is to synthesized and characterize new iron(III) carboxylate precursors for Fe<sub>2</sub>O<sub>3</sub>. We have an on-going interest in the coordination chemistry of new heterocyclic carboxylic acids. Our latest studies focus on the structural characterization and coordination of asymmetrically substituted 2,5-dimercapto-1,3,4-thiadiazole (dmt) derivatives. Our interest for the asymmetric substitution of the dmt heterocycle is in preserving the diversity of donor atoms (N, O, S), which may lead to structural diversity in both coordination chemistry and materials chemistry. Thus, we have investigated a series of three new (3*H*-2-thioxo-1,3,4-thiadiazol-5-yl)-thioalkanoic acids, C<sub>2</sub>HN<sub>2</sub>S<sub>3</sub>(CH<sub>2</sub>)<sub>n</sub>COOH, n = 1, 2, 3 (Fig. 1a).<sup>13,14</sup>

The acetic homologue (n = 1) was used in the synthesis of a large series of main group and transition metal complexes, using both mono- and completely deprotonated acid as ligand. Spectroscopic and X-ray diffraction studies

revealed the versatility of the title acid as N-, S- and/or O-donor.<sup>15-18</sup> Some of its complexes with divalent Mn, Co, Ni and Cu were subjected to thermogravimetric analysis in air and the formation of metal oxides was proposed. However, none of these studies identified the thermal decomposition intermediates or confirmed the identity and quality of the final solid powders.<sup>18,19</sup>

Here we report the first synthesis of an iron(III) complex using the new (3*H*-2-thioxo-1,3,4-thiadiazol-5-yl)-thiosuccinic acid (H<sub>3</sub>L) (Fig. 1b), bearing an extended number of donor atoms, along with the vibrational characterization (FT-IR, FT-Raman) of both starting material and product. We also intend to prove that the iron(III) complex is a suitable precursor for iron(III) oxides. In this respect, we describe the thermal decomposition pattern of the precursor using TG/DTA/DTG analysis along with FT-IR spectroscopy and PXRD for solid fractions identification.

## RESULTS AND DISCUSSION

The reaction of (3*H*-2-thioxo-1,3,4-thiadiazol-5-yl)-thiosuccinic acid (H<sub>3</sub>L) with FeCl<sub>3</sub>·6H<sub>2</sub>O in the presence of Et<sub>3</sub>N, in different molar ratios, produced the same iron(III) complex [FeL]·1.5H<sub>2</sub>O, L = (C<sub>2</sub>N<sub>2</sub>S<sub>3</sub>CH(COO)CH<sub>2</sub>COO)<sup>3-</sup> (Scheme 1). More specific, in the attempt to obtain the complex which contains the mono-deprotonated acid as ligand, [Fe(H<sub>2</sub>L)<sub>3</sub>] the reagents were mixed in the molar ratio FeCl<sub>3</sub>:H<sub>3</sub>L:Et<sub>3</sub>N = 1:3:3 (method I). The method failed and the product proved to correspond to the completely deprotonated homologue, as confirmed by microanalysis (Table 1). In order to reproduce the synthesis for [FeL]·1.5H<sub>2</sub>O, the reagents in the molar ratio FeCl<sub>3</sub>:H<sub>3</sub>L:Et<sub>3</sub>N = 1:1:3 were subjected to a similar procedure (method II) with satisfactory results.

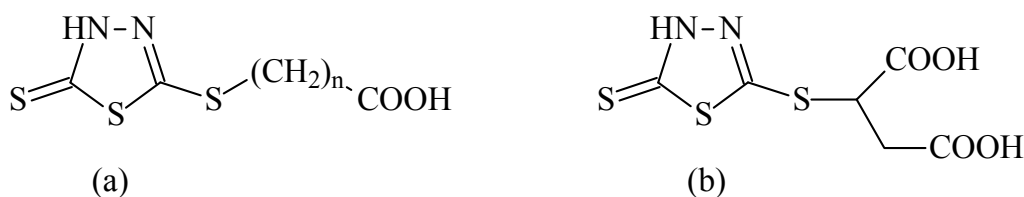
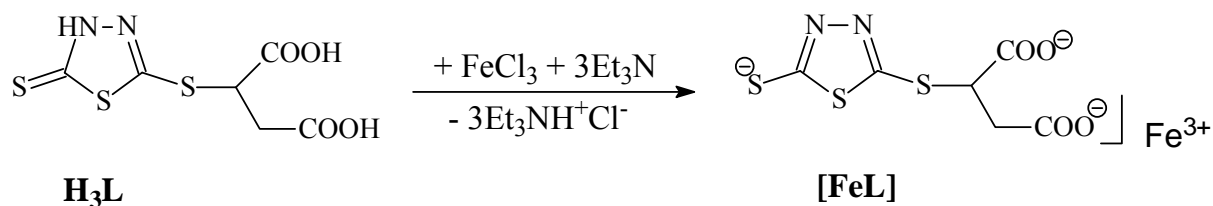


Fig. 1 – Schematic drawing of: (a) 2,5-dimercapto-1,3,4-thiadiazole (dmt), and (b) (3*H*-2-thioxo-1,3,4-thiadiazol-5-yl)-thiosuccinic acid (H<sub>3</sub>L).



Scheme 1

Table 1

The elemental analysis of  $[\text{FeL}] \cdot 1.5\text{H}_2\text{O}$ 

Empirical formula	Molar Weight	% C		% H		% N	
		found	calc.	found	calc.	found	calc.
$\text{C}_6\text{H}_3\text{N}_2\text{S}_3\text{O}_4\text{Fe} \cdot 1.5\text{H}_2\text{O}$	346.167	21.01	20.82	1.86	1.75	7.74	8.09

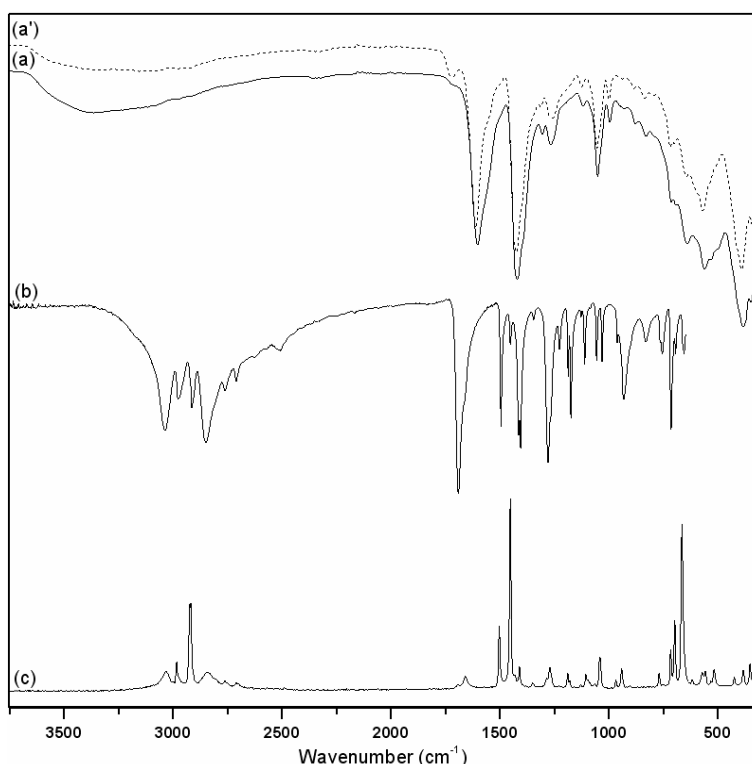


Fig. 2 – Vibrational spectra: (a), (a') ATR-FT-IR for  $[\text{FeL}] \cdot 1.5\text{H}_2\text{O}$  prepared by method II and I, respectively; (b) ATR-FT-IR for  $\text{H}_3\text{L}$ ; (c) FT-Raman for  $\text{H}_3\text{L}$ .

The syntheses were performed in aqueous media for ecological reasons. Triethylamine was used to deprotonate the acid and to increase its solubility in water. The complex  $[\text{FeL}]$  precipitated each time as brown solid and proved stable in open atmosphere, at room temperature. As the product is insoluble in water and common organic solvents, further investigations were carried out in solid state.

#### Vibrational spectroscopic characterization of the precursor

The FT-IR spectra of the precursor and the corresponding starting acid  $\text{H}_3\text{L}$ , along with the

FT-Raman spectrum of the  $\text{H}_3\text{L}$  are presented in Fig. 2. The IR spectra of  $[\text{FeL}] \cdot 1.5\text{H}_2\text{O}$  were recorded for the complexes prepared by method I and II. As it can be observed, the two spectra are similar. On the other hand, the Raman spectrum of the complex could not be recorded. The most relevant spectral data are listed in Table 2. The following discussion is based on the comparison between the current results and the literature data known for related compounds.<sup>13,15-17</sup>

Table 2

Selected vibrational data (cm<sup>-1</sup>) for [FeL]·1.5H<sub>2</sub>O and H<sub>3</sub>L

H <sub>3</sub> L		[FeL]·1.5H <sub>2</sub> O	Vibrational assignment
Raman	IR	IR	
–	–	3500–3000 w,br	ν(H <sub>2</sub> O)
3037 w	3038 s	–	ν(NH)
2984–2761 w–s	2977–2763 m–s	2970–2914 w,sh	ν(CH <sub>2</sub> ) + ν(CH)
–	1690 vs	–	ν(C=O)
–	–	1605 vs,br	ν <sub>as</sub> (COO) + ν(CN)
1504 m, 1452 vs	1495 s, 1453 w	–	ν(CN)+δ(NH)
1407 w, 1269 w	1404 s, 1280 s	1418 vs, 1270 w	δ(CH <sub>2</sub> )
1043 mw	1058 m	1053 m	ν <sub>as</sub> (S–C=S)
721 mw	715 s	714 sh	ν <sub>as</sub> (CSC) <sub>endo</sub>
669 vs	667 w	640 sh	ν <sub>s</sub> (CSC) <sub>endo</sub>

Abbreviations: w – weak, m – medium, s – strong, vs – very strong, br – broad, sh – shoulder, ν – stretching, ν<sub>as</sub> – asymmetric stretching, ν<sub>s</sub> – symmetric stretching, δ – bending, endo-endocyclic.

The IR and Raman spectra of H<sub>3</sub>L are comparable with those of homologue (3*H*-2-thioxo-1,3,4-thiadiazol-5-yl)-thioalkanoic acids, C<sub>2</sub>HN<sub>2</sub>S<sub>3</sub>(CH<sub>2</sub>)<sub>n</sub>COOH, n = 1, 2 and 3.<sup>13</sup> As a consequence, the length and configuration of the thioalkanoic fragment does not influence significantly the vibrational behaviour of these compounds.

The spectra of H<sub>3</sub>L show relevant bands for both heterocyclic and thiosuccinic units. The heterocycle is well represented by the characteristic bands assigned to the CN and CS vibrational modes. More specific, the ν(C=N) fundamental is significantly influenced by the presence of the NH proton. As a result, the characteristic ν(CN)+δ(NH) modes assigned in the 1500–1450 cm<sup>-1</sup> spectral range disappear in the spectrum of [FeL] due to the NH deprotonation. Similarly, the ν(NH) vibrational mode assigned in the spectra of H<sub>3</sub>L at 3038 cm<sup>-1</sup> is missing in the spectrum of the complex. It is important to point out that the protonated heterocycle is present in solid state as thione tautomer. This supposition is supported not only by the assignment of the ν(NH) vibrational mode, but also by the lack of the characteristic ν(SH) bands, usually assigned at 2600–2400 cm<sup>-1</sup> in both IR and Raman spectra.<sup>13</sup> Other important vibrational modes of the heterocycle are located in the approx. 1060–640 cm<sup>-1</sup> spectral range and involve stretching of endo- and exocyclic CS bonds.

The thiosuccinic pendant arm can be characterized by the vibrational modes of the CH<sub>n</sub> and COOH groups. The most intense IR band is

assigned at 1690 cm<sup>-1</sup> and describes the ν(C=O) fundamental. It is well known that the deprotonation of the carboxylic group may produce a significant shift of the ν(C=O) band towards lower wavenumbers, due to the electron delocalization over the carboxylate unit.<sup>20</sup> In our case, the ν<sub>as</sub>(COO) mode is shifted in the IR spectrum of [FeL]·1.5H<sub>2</sub>O by 85 cm<sup>-1</sup>. Unfortunately, it is difficult to assigned the ν<sub>s</sub>(COO) mode due to increased number of IR bands in a relatively narrow spectral range. Similar vibrational behavior was described for the salts and metal complexes of (3*H*-2-thioxo-1,3,4-thiadiazol-5-yl)-thioacetic acid.<sup>15-17</sup>

In addition to the above discussion, it is worth mentioning the presence of a very broad band assigned at approx. 3500 – 3000 cm<sup>-1</sup> to the ν(H<sub>2</sub>O) fundamentals, which proves the hydration of the complex molecule.

### Thermal studies on the precursor

The thermal stability of the iron(III) complex was studied by thermogravimetric analysis. The simultaneous TG/DTA/DTG curves recorded in air are presented in Fig. 3. The summary of TG/DTA/DTG characteristics is given in Table 3. The experimental and calculated data are in good agreement, except for step IV, which reveals a larger mass loss than calculated. In this case, a supplementary mass loss with the evolved gases and/or air flow can be suspected.

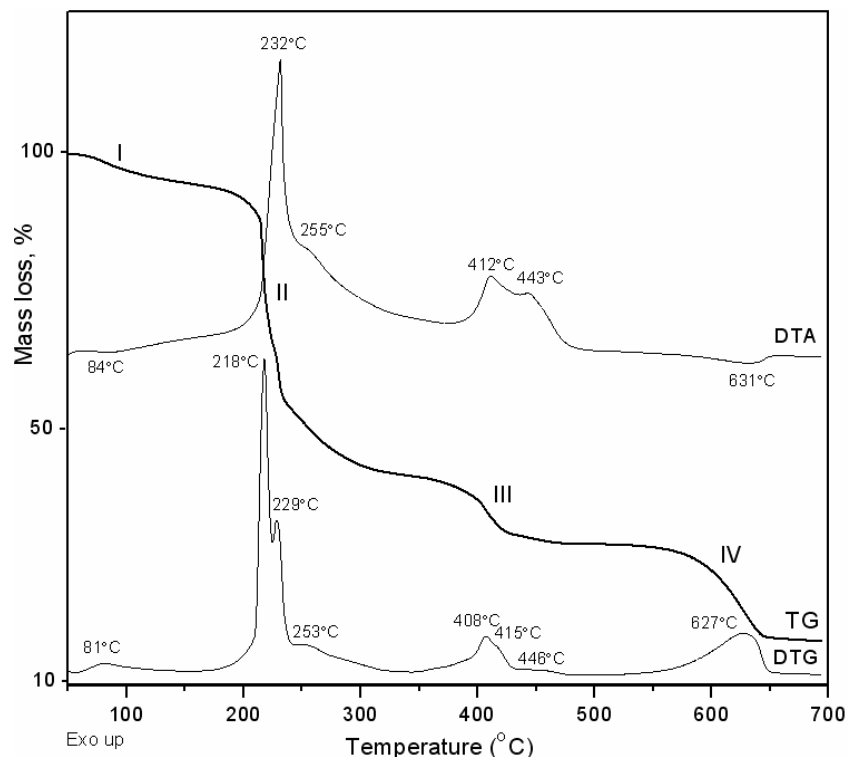


Fig. 3 – Simultaneous TG/DTA/DTG curves of  $[\text{FeL}] \cdot 1.5\text{H}_2\text{O}$  recorded in air at  $10^\circ\text{C}/\text{min}$ .

Table 3

Summary of TG/DTA/DTG characteristics for of  $[\text{FeL}] \cdot 1.5\text{H}_2\text{O}$

Step	Temp. range (°C)	DTA (°C)	DTG (°C)	Residue			Mass loss			
				% exp.	% calc.	Solid	% exp.	% calc.	Gas	
I	50 – 150	84 endo	81	91.83	92.19	$[\text{FeL}]$	8.17	7.80	$1.5\text{H}_2\text{O}$	
II	180 – 340		218	44.06	43.93	$\text{FeSO}_4$	46.49	Combustion gases		
			232 exo							229
			255 exo							253
III	340 – 480		408	32.80	34.68	$\frac{1}{2} \text{Fe}_2\text{O}_2\text{SO}_4$	11.26	11.56	$\frac{1}{2} \text{SO}_3$	
			412 exo							415
			443 exo							446
IV	550 – 650	631 endo	627	17.53	23.12	$\frac{1}{2} \text{Fe}_2\text{O}_3$	15.27	11.56	$\frac{1}{2} \text{SO}_3$	

The TG curve shows an initial continuous weight loss (I) in the  $50\text{--}150^\circ\text{C}$  temperature range, which is consistent with the removal of 1.5 molecules of water. The dehydration process corresponds to a weak endothermic effect. Above  $180^\circ\text{C}$  the anhydrous complex undergoes a massive mass loss (II) caused by the oxidative decomposition of the organic ligand. The process is strongly exothermic and consists of mainly three chemical transformations revealed by the DTG peaks in the  $218\text{--}253^\circ\text{C}$  range. The resulting solid residue formed at  $340^\circ\text{C}$  corresponds to  $\text{FeSO}_4$ . As it concerns the evolved gases, we can only assume the formation of combustion products  $\text{EO}_2$ ,  $\text{E} = \text{C}, \text{S}, \text{N}$ . Despite the combustion of the organic

moiety, the  $\text{Fe(III)}$  undergoes reduction to  $\text{Fe(II)}$ . This behavior is also supported by literature data. For example,  $\text{Fe(III)}$  oxalate undergoes reduction to the  $\text{Fe(II)}$  homologue, followed by oxidation to  $\text{Fe}_3\text{O}_4$  or  $\text{Fe}_2\text{O}_3$ .<sup>21</sup>

Further,  $\text{FeSO}_4$  re-oxidizes shortly above  $340^\circ\text{C}$  (III) to produce the iron(III) oxysulfate,  $\text{Fe}_2\text{O}_2\text{SO}_4$  which remains stable up to  $550^\circ\text{C}$ . The process is less exothermic than the previous one and involves several reactions revealed by the complex, broad DTG peak centered at  $408^\circ\text{C}$ . The last mass loss (IV) corresponds to the endothermic decomposition of  $\text{Fe}_2\text{O}_2\text{SO}_4$ . The final solid residue can be assigned to  $\text{Fe}_2\text{O}_3$  according to FT-IR and PXRD measurement. According to

literature, transformations involving  $\text{Fe}_2\text{O}_3$  formation *via* various oxysulfate intermediates are characteristic for anhydrous iron(II) sulfate during calcination.<sup>22,23</sup> Some global reactions occurring during  $[\text{FeL}]\cdot 1.5\text{H}_2\text{O}$  calcination can be described by the general equations 1-4.

The identity of the solid residues at different temperatures was monitored by FT-IR spectroscopy. The ATR-FT-IR spectra of the hydrated precursor  $[\text{FeL}]\cdot 1.5\text{H}_2\text{O}$  and its calcination products are presented in Fig. 4.

The FT-IR spectra of the (20°C) and (100°C) samples are comparable, which proves that only dehydration occurs at this temperature. However, the presence of  $\nu(\text{H}_2\text{O})$  as a much weaker broad band (3500–3000  $\text{cm}^{-1}$ ) in the spectrum of (100°C) sample indicates that this temperature is not sufficient to complete dehydration. By heating the precursor up to 340°C, the organic mass is

eliminated almost completely, which is confirmed by the dramatic reduction in intensity of the characteristic IR bands. On the other hand, a new, very strong and broad band appears in the 1200–1000  $\text{cm}^{-1}$  spectral range, where  $\nu(\text{SO}_4^{2-})$  fundamentals can be assigned.<sup>20</sup> The same  $\nu(\text{SO}_4^{2-})$  band is present in the IR spectrum of an organic mass free (500°C) sample. These data support the formation of the iron sulfate and oxysulfate during calcinations, as suggested by thermogravimetry. Finally, for the (700°C) sample, the spectrum reveals the characteristic vibrational band of  $\alpha$ - $\text{Fe}_2\text{O}_3$  (hematite).<sup>24</sup>

The formation of hematite as final calcinations product at 700°C was also emphasized by PXRD measurements. The X-ray diffraction pattern of the solid residue (Fig. 5) reveals the single crystalline phase of  $\alpha$ - $\text{Fe}_2\text{O}_3$  (hematite) (JCPDS 89e598).<sup>25</sup>

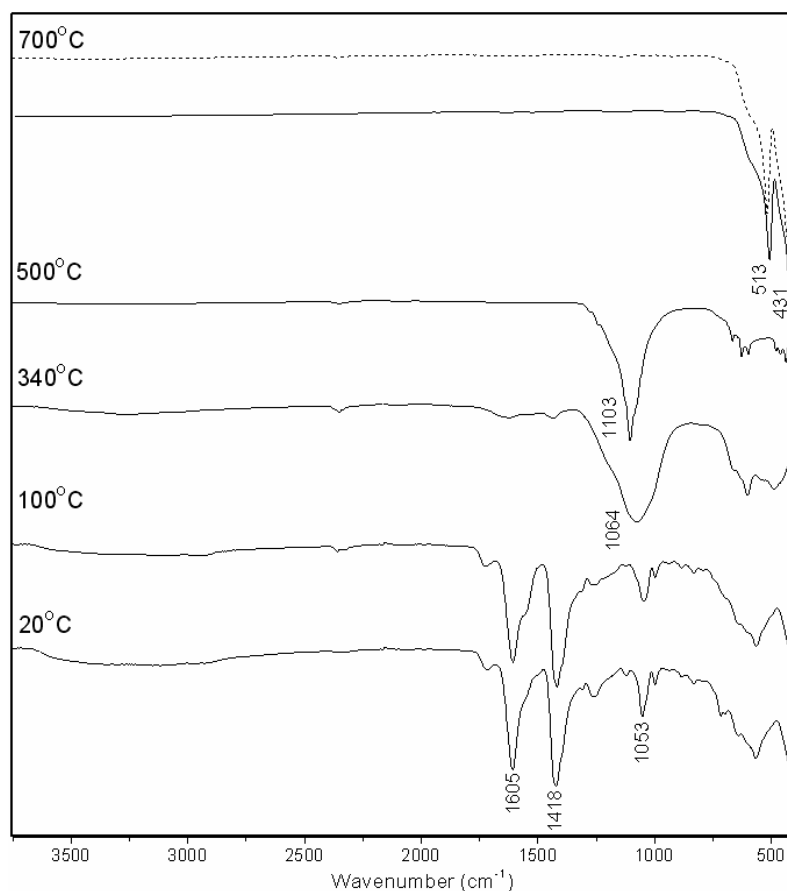


Fig. 4 – FT-IR spectra of  $[\text{FeL}]\cdot 1.5\text{H}_2\text{O}$  (20°C) and its calcination products (100, 340, 500 and 700°C). For 700°C: calcination of the precursor prepared by method I (dot line), and method II (solid line), respectively.

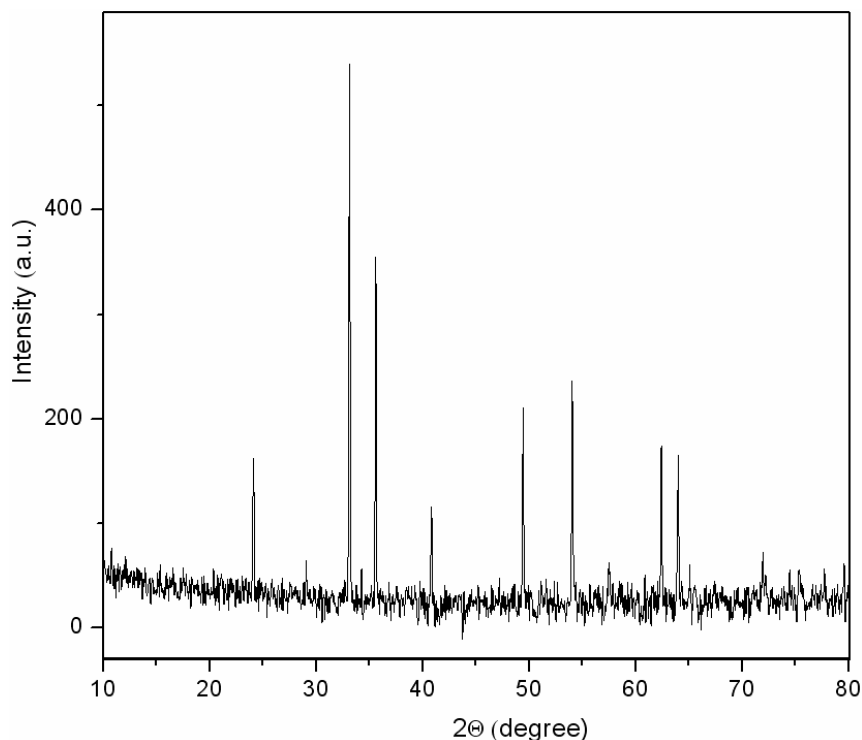


Fig. 5 – X-ray diffraction pattern of the calcinations product at 700°C.

## EXPERIMENTAL

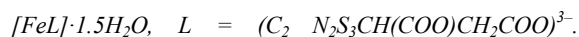
### Materials and methods

The starting materials were purchased from commercial sources as analytical pure reagents and were used with no further purification. All experiments were performed in open atmosphere. The preparation method for (3*H*-2-thioxo-1,3,4-thiadiazol-5-yl)-thiosuccinic acid ( $H_3L$ ) was reported elsewhere.<sup>13</sup>

Elemental analyses were obtained on a VarioEL apparatus from Elementar Analysensysteme GmbH. Melting points (uncorrected) were measured in the 30–360°C range using a KRUSS KSPI digital apparatus. The FT-Raman spectrum on solid  $H_3L$  (4000–200  $cm^{-1}$ ) was recorded at room temperature, using an Equinox 55 Bruker spectrometer with an integrated FRA 106 S Raman module. The excitation of the Raman spectrum was performed using the 1064 nm line from a Nd:YAG laser with an output power of 250 mW. An InGaAs detector operating at room temperature was used. The ATR-FT-IR spectrum of  $H_3L$  (3750–650  $cm^{-1}$ ) was recorded on the same spectrometer by coupling an ATR MIRacle module with ZnSe contact crystal. The spectral resolution was 2  $cm^{-1}$ . ATR-FT-IR spectra of solid  $[FeL] \cdot 1.5H_2O$  and corresponding decomposition residues (4000–300  $cm^{-1}$ ) were recorded using a Bruker Tensor 27 Spectrophotometer with Platinum ATR (single reflection diamond ATR) module. The spectra were collected with a 4  $cm^{-1}$  spectral resolution and 32 scans. Thermogravimetric analysis (TG/DTA/DTG) was carried out on a SDT Q 600 Universal V4.5A TA Instruments apparatus. The sample with mass of 7.4560 mg was placed in alumina crucible and heated non-isothermally from 30°C to 700°C with a heating rate of 10°C/min, under an air flow of 100 mL/min. Thermal decomposition of larger samples was carried out in a Nabertherm 30-3000°C chamber furnace. Powder X-Ray Diffraction (PXRD) was carried out at room

temperature, on a Bruker D8 Advance diffractometer, with a Ge (111) monochromator in the incident beam Cu-K $\alpha$ 1 radiation ( $\lambda = 1.54056 \text{ \AA}$ ), having the source power of 40kV and 40mA. Experimental files were visualized and drawings were created with the ORIGIN graphing and data analysis software package.<sup>26</sup>

### Synthesis



*Method I:* In the attempt to obtain the iron(III) complex containing the mono-deprotonated acid as ligand,  $[Fe(H_2L)_3]$  the reaction produced the completely deprotonated homologue,  $[FeL]$ . Thus, an orange solution of  $FeCl_3 \cdot 6H_2O$  (0.14 g, 0.5 mmol) in 2 mL distilled water was added dropwise to an aqueous solution of  $H_3L$  (0.40 g, 1.5 mmol) and  $Et_3N$  (0.21 mL, 1.5 mmol; 0.73  $g/cm^3$ ) in 5 mL distilled water, under continuous stirring. The product deposited at once as brown powder. After stirring the reaction mixture for 30 min. at room temperature, the product was filtered and washed with distilled water, then dried at room temperature, in open atmosphere. The limitative amount of  $FeCl_3 \cdot 6H_2O$  was used in yield calculation. Yield 94.1%; mp = 253–5°C (decomposition).

*Method II:* The synthesis of  $[FeL] \cdot 1.5H_2O$  was reproduced with the right stoichiometry. Thus,  $FeCl_3 \cdot 6H_2O$  (0.54 g, 2 mmol) dissolved in 5 mL distilled water and  $H_3L$  (0.53 g, 2 mmol) and  $Et_3N$  (0.83 mL, 6 mmol) dissolved in 20 mL distilled water were mixed as previously described. Yield 94.2%; mp = 253–5°C (decomposition).

*Thermolysis products:* Four samples of  $[FeL] \cdot 1.5H_2O$  were placed in ceramic crucibles and calcinated at different temperatures for 2 hours, with a heating rate of 5°C/min: 100°C (0.010 g), 340°C (0.022 g), 500°C (0.030 g) 0.040 g (700°C). In order to verify the reproducibility, another sample of 0.552 g precursor was calcinated at 700°C for 4 hours. The

Fe<sub>2</sub>O<sub>3</sub> resulted at 700°C as brownish-red solid residue, in quantitative yield.

## CONCLUSIONS

The new iron(III)-organic precursor [FeL]·1.5H<sub>2</sub>O can be synthesized from the corresponding acid H<sub>3</sub>L by complete deprotonation, as proved by microanalysis and vibrational spectroscopy. The homologue complex containing the mono-deprotonated acid as ligand could not be obtained. The TG/DTA/DTG analysis shows that the precursor undergoes thermal decomposition in air in four major steps: dehydration, organic mass combustion, iron(II) sulfate oxidation and iron(III) oxysulfate decomposition, respectively. All the resulting solid residues are identified by FT-IR spectroscopy. In addition, the final product α-Fe<sub>2</sub>O<sub>3</sub> is confirmed by PXRD analysis.

Our current work shows the ability of this new ligand (H<sub>3</sub>L) to form an iron complex which is a suitable metal-organic precursor for iron(III) oxides. Further work is required in order to gain more information on both material and precursor. Thus, size and morphology of the α-Fe<sub>2</sub>O<sub>3</sub> particles will be established by electronic microscopy. Moreover, new related precursors will be prepared by tuning the ligand, and the influence of variable ligand molecular structure on the thermal decomposition pattern and produced material will be investigated.

*Acknowledgements:* Financial support from National University Research Council of Roumania (Research Project PNII-ID 0659/2011) is greatly appreciated. MMV thanks Prof. Dr. Lelia Ciontea and Dr. Simona Pinzaru for facilitating the FT-IR and FT-Raman measurements.

## REFERENCES

1. E. Esmailia, M. Salavati-Niasaria, F. Mohandesb, F. Davara and H. Seyghalkarb, *Chem. Eng. J.*, **2011**, *170*, 278.
2. M. Stefanescu, O. Stefanescu, M. Stoia and C. Lazau, *J. Therm. Anal. Calorim.*, **2007**, *88*, 27.
3. O. Stefanescu and M. Stefanescu, *J. Organomet. Chem.*, **2013**, *740*, 50.
4. B. Mao, Z. Kang, E. Wang, C. Tian, Z. Zhang, C. Wang, Y. Song and M. Li, *J. Solid State Chem.*, **2007**, *180*, 489.
5. W.-W. Wang, Y.-J. Zhu and M.-L. Ruan, *J. Nanopart. Res.*, **2007**, *9*, 419.
6. X. Hu, J.C. Yu, J. Gong, Q. Li and G. Li, *Adv. Mater.*, **2007**, *19*, 2324.
7. J. Pinkas, V. Reichlova, R. Zboril, Z. Moravec, P. Bezducka and J. Matejkova, *Ultrason. Sonochem.*, **2008**, *15*, 257.
8. F. Ozel, H. Kockar, S. Beyaz, O. Karaagac and T. Tanrisever, *J. Mater. Sci.: Mater. Electron.*, **2013**, *24*, 3073.
9. R.C. Chikate, K.-W. Jun and C.V. Rode, *Polyhedron*, **2008**, *27*, 933.
10. G. Zhang, K. Shen, D. Zhao, Y. Yuan and G. Wang, *Mater. Lett.*, **2008**, *62*, 219.
11. M.Y. Masoomi and A. Morsali, *Coord. Chem. Rev.*, **2012**, *256*, 2921.
12. A. Ganguly, R. Kundu, K.V. Ramanujachary, S.E. Lofland, D. Das, N.Y. Vasanthacharya, T. Ahmad and A.K. Ganguli, *J. Chem. Sci.*, **2008**, *120*, 52.
13. M.M. Venter, S. Cinta Pinzaru, I. Haiduc and V. Bercean, *Studia Univ. Babeş-Bolyai, Physica*, **2004**, *XLIX*, 285.
14. A.E. Pascui, M.M. Venter and V.N. Bercean, *Studia Univ. Babeş-Bolyai, Ser. Chem.*, **2009**, *LIV*, 68.
15. M.M. Venter, V. Chis, S. Cinta Pinzaru, V.N. Bercean, M. Ilici and I. Haiduc, *Studia Univ. Babeş-Bolyai, Ser. Chem.*, **2006**, *LI*, 65.
16. M.M. Venter, A. Pascui, V.N. Bercean and S. Cinta Pinzaru, *Studia Univ. Babeş-Bolyai, Ser. Chem.*, **2007**, *LII*, 55.
17. M.M. Venter, V.N. Bercean, M. Ilici and S. Cinta Pinzaru, *Rev. Roum. Chim.*, **2007**, *52(1-2)*, 75.
18. M.M. Venter, V.N. Bercean, R.A. Varga, V. Sasca, T. Petrişor jr. and L. Ciontea, *Studia Univ. Babeş-Bolyai, Ser. Chem.*, **2010**, *XLV, TOM II*, 217.
19. M. Ilici, V. Bercean, M. Venter, I. Ledeti, T. Olariu, L.-M. Şuta and A. Fuliş, *Rev. Chim.*, **2014**, *65(10)*, 1142.
20. K. Nakamoto, "Infrared and Raman Spectra of Inorganic and Coordination Compounds", vol. A and B, 6<sup>th</sup> Edition, Wiley, New Jersey, 2009.
21. V. Berbenni, C. Milanese, G. Bruni, A. Marini and I. Pallecchi, *Thermochim. Acta*, **2006**, *447*, 184.
22. M. Foldvari, "Handbook of thermogravimetric system of minerals and its use in geological practice", Geological Institute of Hungary, Budapest, 2011, p. 124.
23. A.K. Galwey and M.E. Brown, "Thermal Decomposition of Ionic Solids: Chemical Properties and Reactivities of Ionic Crystalline Phases", Elsevier, Amsterdam, 1999, p. 400.
24. H. Namduri and S. Nasrazadani, *Corros. Sci.*, **2008**, *50*, 2493.
25. Joint Committee on Powder Diffraction Standards, International Center for Diffraction Data, Swarthmore, 1993.
26. ORIGIN – Graphing and Data Analysis Software Package, OriginLab Corporation, One Roundhouse Plaza, Northampton, MA 01060 USA, 2008.